7.3.4 Clamp conformation during initial RNA synthesis

A previous single-molecule confocal spectroscopy study produced results suggesting that the clamp does not open during *de novo* RNA synthesis (27). However, as this study was not able to monitor molecules in real-time, it remained a possibility that transient or partial clamp opening events occurred during RNA synthesis but were not captured. Using TIRF microscopy and building upon the success we have had in observing real-time RNA synthesis (see chapter 6), we are able to confirm that clamp opening does not occur during RNA synthesis.

We immobilized pre-formed RP_O (using fully complementary DNA) and added NTP reaction mixtures to the observation chamber during data acquisition. In one experiment our NTP reaction mixture permitted the synthesis of short RNAs up to 7-nt in length ($RP_{ITC\leq7}$). In a second experiment, our NTP mixture permitted the synthesis of RNAs up to 11-nt in length (RD_{e11}). In the RD_{e11} experiment, it was expected that some molecules would escape the promoter and form stable elongation complexes. We performed experiments at both 20 and 200 ms temporal resolutions but failed to see any indications of clamp opening – fully or partially – upon the addition of the NTP reaction mixtures (Fig. 7.8). In addition, no FRET transitions were observed in these experiments.

Our observations suggest that each nucleotide addition cycle is not accompanied by a clamp opening and closing cycle, and that RNAP translocates along the promoter DNA during initial RNA synthesis with the clamp in a closed conformation. We propose that it is this closed clamp conformation that confers processivity to the transcribing RNAP. Our results also suggest that the clamp remains closed during the release of abortive RNAs. This leaves the NTP-entry channel as the only possible route through which abortive RNAs might be released. We note that our 20 ms temporal resolution data is not able to eliminate the possibility that each nucleotide addition cycle is accompanied by clamp opening and closing cycles that occur on faster timescale than the temporal resolution afforded by our assay. However, in agreement with our

findings, earlier solution confocal studies with 1 ms temporal resolution also failed to detect clamp opening and closing transitions during RNA synthesis (27).

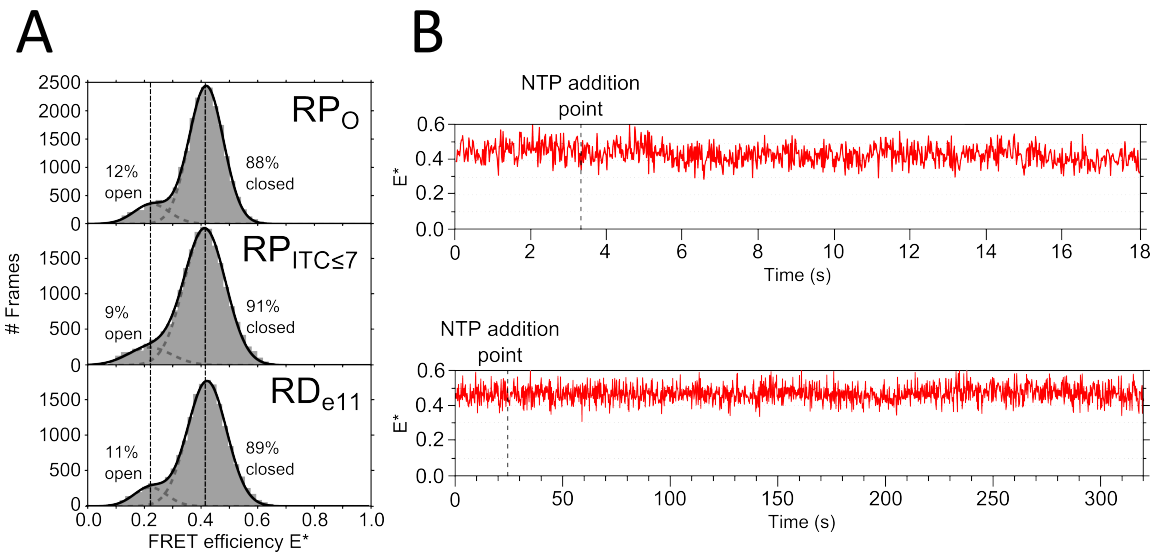


Figure 7.8. RNAP clamp conformation during initial RNA synthesis. (A) Stacked E* histograms and Gaussian fits for immobilized RP_O (top), $RP_{ITC≤7}$ (middle), and RD_{e11} (bottom). Temporal resolution is 20 ms. 100 molecules contribute to each histogram. (B) Example time trajectories showing no change in FRET upon the addition of the NTP reaction mixture. Top figure shows 20 ms temporal resolution data; bottom figure shows 200 ms temporal resolution data. The NTP addition time point is marked with a dashed line.

7.3.5 Effect of switch-region-target inhibitors on the RNAP clamp conformation

The RNAP switch region is located at the base of the RNAP clamp and is considered an important antibiotic target (123, 203). Recently, it was shown that a number of switch-region-target inhibitors modulate the RNAP clamp conformation. In this section, we show what affect the switch-region-target inhibitors, Myxopyronin (Myx) and Lipiarmycin (Lpm), have on the RNAP clamp conformation using our smFRET assay.

In a first set of experiments, we incubated RNAP holoenzyme with Myx to form an RNAP-Myx complex. These complexes were immobilized on a PEG-passivated surface and imaged using TIRF microscopy in imaging buffer supplemented with 20 µM of Myx. The resulting E* histogram showed that Myx depopulates the open clamp conformation

and stabilises the closed clamp conformation (Fig. 7.9A). Real-time Myx binding experiments to test whether the effect of Myx on the clamp conformation was immediate upon binding were then carried out. The time trajectory data showed that if the clamp was in a closed conformation, no change was observed when Myx was added; however, if the clamp was in a stable open conformation, Myx binding appeared to induce clamp closure (Fig. 79B–C). Interestingly, if the clamp was exhibiting dynamics, Myx binding also appeared to induce stable clamp closure (Fig. 7.9C). We note however, that clamp closing did not occur in a highly synchronous manner across all molecules; in fact, in some cases, the delay lasted up to many tens of seconds. This asynchrony is reflected in Fig. 7.9B.

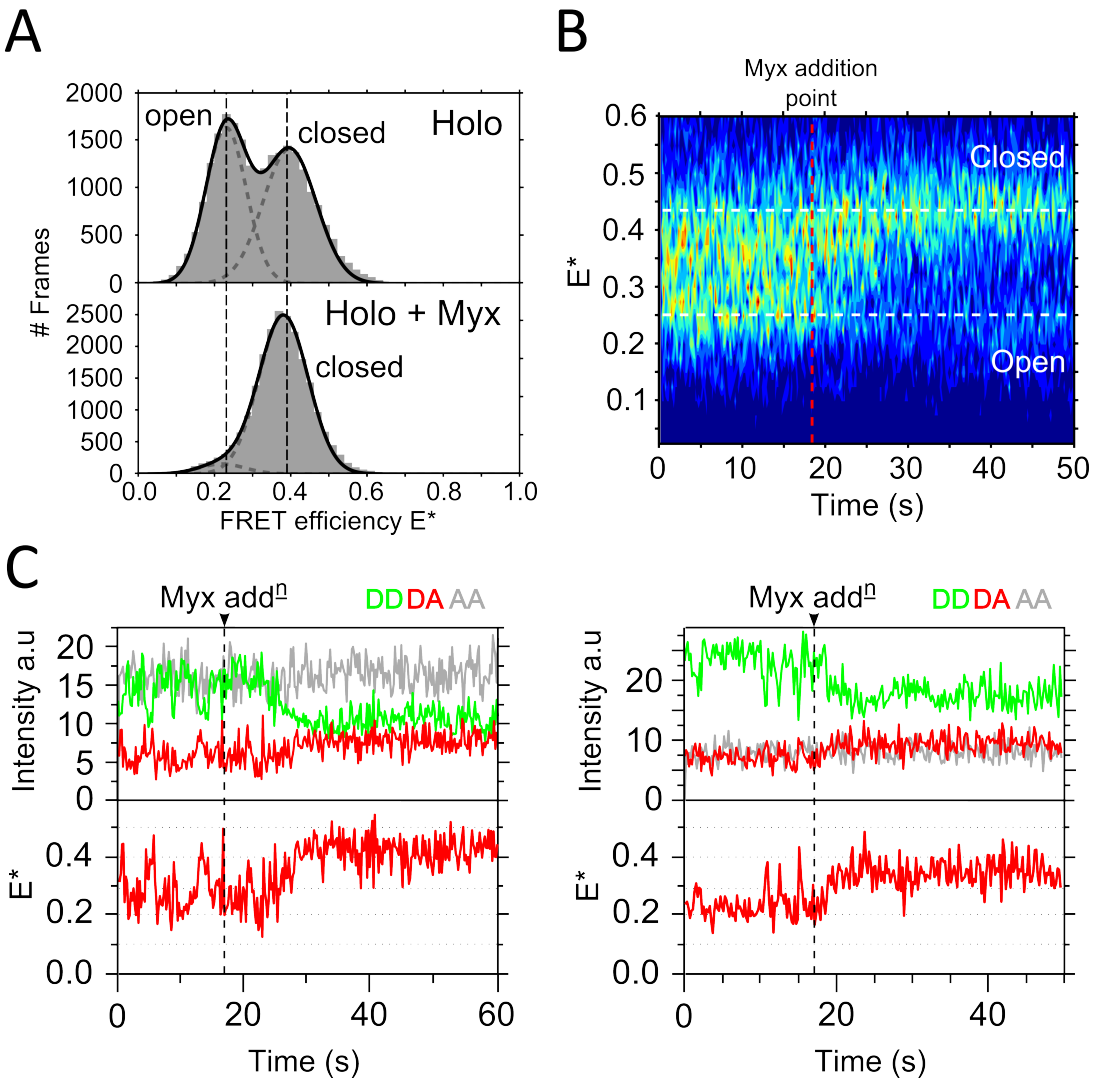


Figure 7.9 RNAP clamp response to Myxopyronin. (A) Stacked E* histograms of RNAP holoenzyme (top), and holoenzyme in the presence of 20 µM Myx (bottom). Temporal resolution is 20ms. Each histogram shows data of 100 molecules. (B) Heat map of the E*

distributions of FRET time trajectories in a single field-of-view. Blue to red colours represent an increasing number of events. 48 molecules are shown. (C) Example time trajectories of fluorescence intensities and E* traces showing clamp closing upon the addition of Myx to the observation chamber. Data in B–C was taken at a temporal resolution of 200ms.

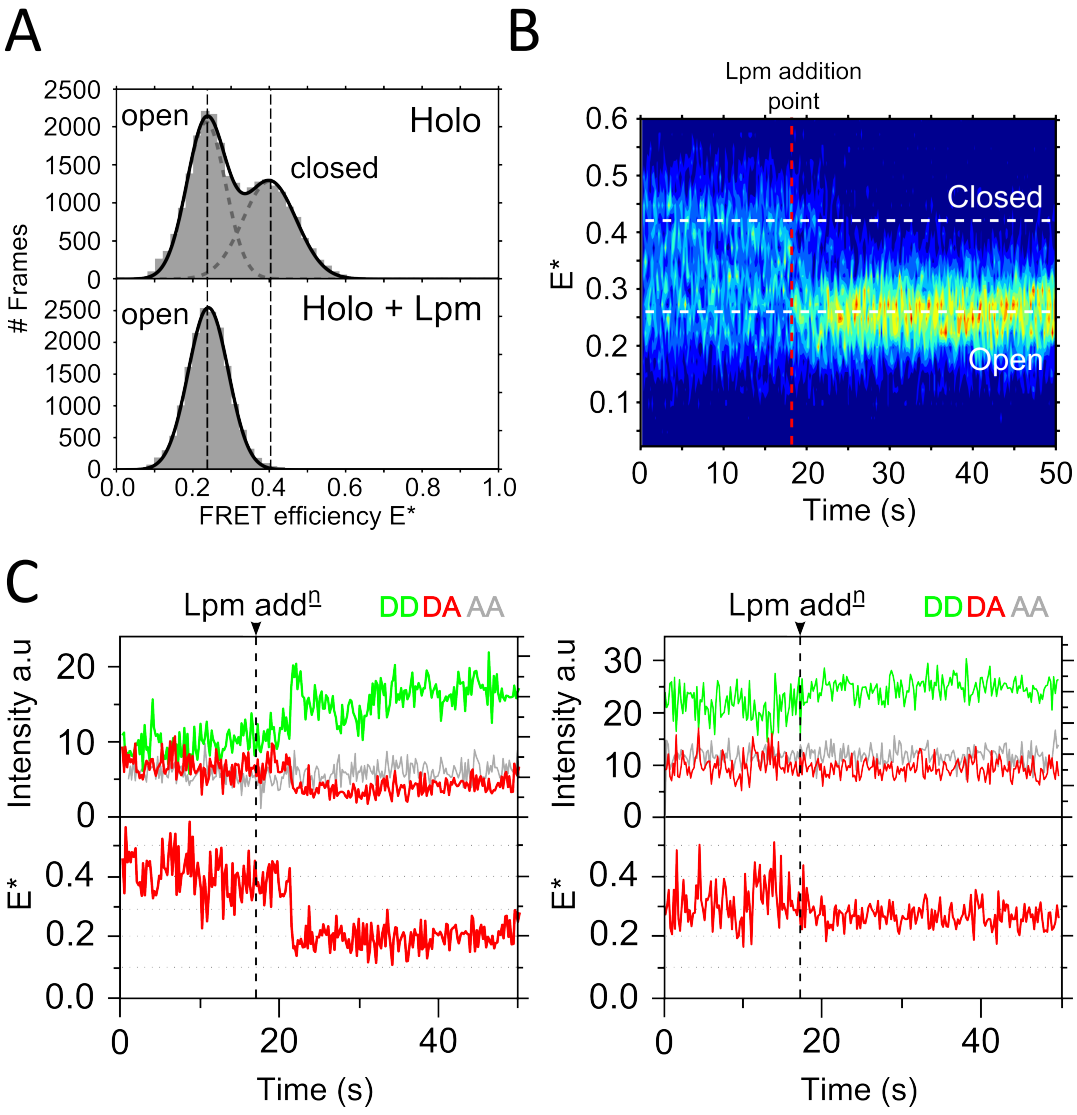


Figure 7.10. RNAP clamp response to Lipiarmycin. (A) Stacked E* histograms of RNAP holoenzyme (top), and holoenzyme in the presence of 20 µM Lipiarmycin (bottom). Temporal resolution is 20ms. Each histogram shows data of 100 molecules. (B) Heat map of the E* distributions of FRET time trajectories from a single field-of-view. Blue to red colours represent an increasing number of events. 55 molecules are shown. (C) Example time trajectories of fluorescence intensities and E* traces showing clamp opening upon the addition of Lpm to the observation chamber. Data in B–C was taken at a temporal resolution of 200ms.

Next, we performed the same experiments described above, this time using Lpm as the inhibitor. Interestingly, the E* histogram of RNAP-Lpm complexes showed that Lpm depopulates the closed clamp conformation and stabilises the open clamp conformation (Fig. 7.10A). Real-time binding experiments showed that Lpm was able to induce clamp opening in molecules that had either a stable closed clamp conformation or the clamp undergoing opening and closing transitions (Fig. 7.10B–C); Lpm binding appeared to have no effect on molecules that already had a stable open clamp conformation. Interestingly, and in contrast to Myx binding-induced clamp closure, clamp opening upon Lpm binding appears to be highly synchronous (Fig. 7.10B–C). Although having said this, a number of molecules did show clear delayed responses to Lpm of up 3 seconds (Fig. 7.10C).

There are a number of possible explanations for this delay in response. The first is incomplete mixing when the inhibitor is added to the well. We believe this is unlikely considering the fact that the difference in synchrony between Lpm and Myx was reproducible between experiments. The addition of Lpm invariably led to a well synchronised decrease in FRET. The addition of Myx invariably led to an asynchronous increase in FRET. We suggest that if the asynchrony was simply due to mixing, the delayed FRET change upon the addition of Lpm and Myx would be similar; hence we suggest that mixing is not the main factor producing this asynchronous FRET change. A second possible explanation is that it takes longer for Myx to diffuse to its binding site compared with Lpm. However, given the fact that the diffusion coefficients of the two inhibitors are both $D_{Myx} \sim 3.4 \times 10^{-10} m^2 s^{-1}$, differences in diffusion times are unlikely to account for the different clamp response times. A third possibility is that the binding sites of the two inhibitors may be situated in different locations. Mutational and structural studies, however, indicate that the Myx and Lpm binding sites partially overlap (204). A fourth possibility is that there is a difference in the accessibility of the binding sites for the two inhibitors. Perhaps the clamp must be in a specific conformation for the inhibitors (especially Myx) to bind? We note that increasing the concentration of Myx 10-fold still produced the delay seen in Fig. 7.9, and supports this

fourth possibility. Future studies using microfluidics to eliminate differences in mixing times will investigate the asynchrony further.

7.4 Discussion

7.4.1 RNAP clamp adopts a primarily open conformation in holoenzyme

A previous single-molecule study showed that the RNAP clamp changes conformation at different stages of the transcription cycle (27). This confirmed a long-standing hypothesis based on RNAP crystal structures that the RNAP clamp is a mobile domain. However, the single-molecule study enabled only short snapshots (~1ms) of the clamp conformation in diffusing RNAP molecules, and therefore did not provide detailed information regarding the kinetics of the presumed clamp opening and closing transitions. In this work, we utilized an Ab-immobilization strategy (see chapter 4) to monitor the RNAP clamp conformation over many seconds.

Our work has revealed that in RNAP holoenzyme, the clamp adopts two conformational states, an open conformation and a closed conformation, with the open being the most populated state (Fig. 7.4A). We propose that the open and closed states are the same as those observed in (27). Our results showed no evidence of a *bona fide* clamp-collapsed state. Our raw FRET data, that is, data before applying selection criteria, showed a population of molecules with E* values higher than that corresponding to the closed clamp conformation (E*>0.5). This population could potentially be interpreted as a clamp-collapsed state; however, we found that data frames that contribute to the E*>0.5 population arise from molecules that display aberrant photophysical behaviour (Fig. 7.5). These molecules could not be used to make reliable biological interpretations, and were therefore discarded from further data analysis. We propose that the earlier confocal spectroscopy study was unable to exclude these molecules from data analysis, which meant they were included in the FRET histograms. Based on this logic, we propose that RNAP holoenzyme does not adopt a clamp-collapsed conformation.

The results described above have implications for the RP_O formation mechanism. There are currently two favoured models for the mechanism of transcription bubble melting: *bend-load-open* and *open-bend-load* (66, 68). In the former, full DNA unwinding occurs after the duplex DNA has entered the DNA binding cleft and is promoted by interactions between the clamp and downstream DNA (76). In the latter, DNA unwinding must occur before the promoter DNA enters the binding cleft (74). Early crystal structures of RNAP holoenzyme alone and holoenzyme bound to a fork-junction promoter DNA fragment showed the clamp in a closed conformation that rendered the DNA binding cleft too narrow to accommodate double-stranded DNA (dsDNA) (49). This led to proposals that promoter DNA enters the binding cleft as single-stranded DNA (ssDNA) and therefore must melt outside of the binding cleft (17, 49). Other studies however, have indicated that transcription bubble opening can occur inside of the cleft (66). Our work shows that the holoenzyme clamp adopts mainly an open conformation, and is therefore able to accommodate dsDNA. This supports a model in which bubble melting can occur inside of the binding cleft.

Our time trajectory data revealed considerable heterogeneity in the clamp conformation among RNAP holoenzyme molecules. Behaviours were classified as open (clamp remains stably open for many seconds), closed (clamp remains stably closed for many seconds), and dynamic (clamp undergoes clear conformational transitions between the open and closed conformations). This heterogeneity was reminiscent of that observed for DNA polymerase I Klenow fragment (KF, see chapter 4). As with KF, it is unclear what gives rise to these differences in behaviour, or if indeed the heterogeneity has any functional importance. Future work involving the vesicle-immobilization of RNAP holoenzyme will confirm that the Ab-immobilization technique is not the cause of the heterogeneity, and will explore possible functions of the heterogeneity.

7.4.2 RNAP clamp is closed in RP_O and remains closed during RNA synthesis

Next, we monitored the clamp conformation in RP_O and tested whether the clamp conformation changes in response to NTPs. We found that the clamp adopted a stable closed conformation in RP_O and showed no change in conformation upon the addition of NTPs at both 20 and 200 ms temporal resolutions. This suggests that the clamp remains fully closed as RNAP translocates along the DNA during initial RNA synthesis. We propose that contacts between the RNAP clamp and promoter DNA are not sufficiently strong to impede forward movement of the polymerase, and that the closed clamp conformation stabilises the RNAP-promoter DNA complex during initial transcription. We highlight that our findings provide new insight into whether or not the RNAP clamp opens to permit RNAP forward movement during RNA synthesis? We can confirm that, at least for the initial stages of RNA synthesis and promoter escape, clamp opening and closing cycles that occur on a slower timescale than the temporal resolution afforded by our studies (20 ms) do not occur.

7.4.3 Switch-region-target inhibitors differentially modulate the clamp conformation

Mutational and biochemical studies have shown that the RNAP switch region is the target for a number of small molecule inhibitors including Myx and Lpm. Myx inhibits the RP_C to RP_O transition, which occurs late in the RP_O formation pathway, and is the step at which the transcription bubble opens. Lpm on the other hand inhibits an earlier step in the RP_O formation pathway (68). A previous single-molecule fluorescence study revealed that Myx binding to the RNAP switch region stabilises the closed clamp conformation. Based on this finding, the authors proposed that Myx-induced clamp closure prevents the entry of DNA into the active centre cleft, and therefore inhibits RNAP function by preventing the formation of RP_O (27). Investigations into the inhibition mechanism of Lpm have raised the possibility that Lpm stabilises the open clamp conformation (68, 80), however, this has yet to be shown directly.

In the work presented in this chapter, we showed that Myx stabilises the closed clamp conformation by inducing RNAP clamp closure upon binding to RNAP (Fig. 7.9). In addition, we showed that Lpm binding to RNAP induces clamp opening (Fig. 7.10). However, in both cases a proportion of molecules show a delayed response to inhibitor binding. Our results also indicated that neither RNAP-Myx nor RNAP-Lpm complexes exhibit clamp conformational dynamics i.e. the clamp is locked in a closed or open conformation, respectively. Our findings support the hypothesis that Myx and Lpm function by a hinge-jamming mechanism in which they lock the clamp in a single conformation, which prevents RNAP from proceeding along the transcription initiation pathway (123). It is interesting that inhibitors that bind to the same general switch region of RNAP can have very different effects on the RNAP clamp conformation; Lpm induces a stable open clamp state while Myx induces a stable closed clamp state. This suggests that both the open and closed conformations are functionally important in the transcription mechanism, which leads us to speculate that both conformations are obligatory intermediates in transcription initiation.

The fact that Myx appears to inhibit the RP_C to RP_O transition by locking the RNAP clamp in a closed conformation strongly suggests that transcription bubble melting necessarily occurs inside the DNA binding cleft. This is because, if melting could occur outside of the binding cleft, clamp closure would have no or little effect on the RP_C to RP_O transition. We take this observation as further support for a model in which transcription bubble opening occurs inside of the DNA binding cleft.

7.4.4 Integrating work from different chapters to understand the RP_O formation mechanism

The results presented in chapter 5 demonstrated that the transcription bubble readily undergoes opening and closing transitions even once a stable heparin-resistant complex has been formed at the *lac* promoter. The work presented in this chapter showed that the clamp remains stably closed once a heparin-resistant complex has been formed. These observations suggest that bubble opening and closing is independent of

the clamp conformation, and presumably occurs when promoter DNA is loaded inside of the DNA binding cleft. This, combined with the observations that holoenzyme adopts primarily an open clamp conformation, and Myx inhibits transcription bubble opening by inducing clamp closure, support a model in which transcription bubble opening occurs inside of the DNA binding cleft. We note however that our experiments do not monitor the clamp and bubble conformations in real-time from initial binding of RNAP to promoter DNA through to RP_O formation. In this situation, it is possible that the order of events (bubble opening and clamp closing) may be different. Future work combining our transcription bubble assay with the clamp conformation assay is needed to determine exactly at which step in the RP_O formation pathway bubble opening and clamp closing occur.

7.5 Conclusion

In this chapter we presented results that shed new light into RNAP clamp conformational dynamics. Our work is the first to demonstrate clamp opening and closing cycles directly, and in doing so confirms earlier proposals that the clamp is a mobile domain. Our work demonstrates that the clamp closes in RP_O and does not open during subsequent stages of transcription initiation. Our investigations have revealed that switch-region-target inhibitors are able to modulate the clamp conformation differentially, which may have implications for the future development of antibiotics. Combined with results presented in earlier chapters, our work provides a detailed view of the protein and DNA conformational changes that occur in transcription initiation. In the future, we intend to extend the investigations presented in this chapter to monitor the transcription bubble and clamp conformations in parallel. These experiments might involve the use of 3-colour or 4-colour FRET to monitor multiple distance changes. This should allow us to address questions such as: when does the clamp close in the RP_O formation pathway? And does clamp closing precede or follow transcription bubble opening? Finally, we note that the work presented in this chapter can be extended to monitor the clamp conformation during elongation and termination.

7.6 Contributions

I performed all work described in this chapter except for the following contributions made by others: Abhishek Mazumder based in Dr. Richard Ebright's group (Rutgers University, USA) purified and labelled RNAP holoenzyme. Geraint Evans (Oxford University, UK) provided custom-written MATLAB code that was modified to visualise data.

Chapter 8: Conclusion

Efforts to investigate transcription initiation using TIRF microscopy have been ongoing for almost a decade in the Kapanidis group. However, there have been many issues encountered during that time, which have delayed progression and limited productivity. In this thesis, we presented two methods to immobilize proteins and protein-DNA complexes for smFRET studies. One involved encapsulating biomolecules within lipid vesicles that were then immobilized in their entirety. The other involved the use of an antibody to anchor proteins of interest to a surface. We successfully applied these immobilization techniques to investigate conformational dynamics in RNAP-promoter DNA complexes. We found that immobilizing RNAP-promoter DNA complexes using the vesicle immobilization technique was technically demanding and therefore less preferential for investigations of the mechanism of RNA synthesis. This being the case, we performed all experiments in chapters 6 and 7 using the antibody-immobilization approach. However, we note that the availability of two independent immobilization strategies will enable us to exclude the possibility that interesting behaviours are artefacts of one or other immobilization strategy in future investigations.

Our investigations into the conformational dynamics of RNAP-promoter DNA complexes showed that the transcription bubble in these complexes undergoes large-scale dynamic fluctuations between states we define as open and closed. This finding shows that the bacterial RNAP, like the mitochondrial and eukaryotic RNA polymerases, exhibits large structural changes in the transcription bubble when bound to promoter DNAs. We speculate that the observed dynamics is functionally important in transcription initiation. Our results also revealed the presence of stable RNAP-promoter DNA complexes that have transcription bubble conformations intermediate between what is expected for the closed complex (RP_C) and the open complex (RP_O). The first intermediate appears to have the bubble in an entirely closed conformation, while a second intermediate has the bubble neither fully open nor fully closed. In short, we

observed considerable static and dynamic heterogeneity and speculate that this heterogeneity may provide an explanation for the heterogeneity in transcription reactions reported in the literature (84, 100).

The underlying cause of the observed heterogeneity is currently unclear. At the most fundamental level, there are two possibilities. The first is that the heterogeneity is an artefact. The second is that the heterogeneity is real and plays some functional role in the bacterial transcription mechanism.

There are a number of potential experimental sources that might lead to the observed heterogeneity being an artefact. Three possibilities are: 1) the fluorophore-stabilising factors added to TIRF experiments (trolox and the oxygen scavenging system), 2) the fact that experiments are performed *in vitro* with a purified enzyme, and 3) experiments are performed using TIRF microscopy after immobilizing the complex of interest. We believe that these explanations for the heterogeneity are unlikely to be true for the following reasons. Firstly, confocal, TIRF, and *in vitro* transcription assay studies performed with and without the fluorophore stabilising factors did not alter our results[20]. Also, approximately the same behaviour was observed when enzymes obtained from different sources were used in our experiments – we tested enzyme preparations prepared by different research groups as well as commercial enzyme samples purified using different purification techniques. This suggests that the purification of the enzyme does not cause the heterogeneity observed. In addition, we immobilized the RNAP-DNA complex for TIRF experiments using two very different immobilization strategies. The antibody (Ab) immobilization approach anchored the protein to the surface directly; the other immobilized the complex by encapsulating it within a vesicle, which was then anchored to the surface. In the vesicle immobilization approach, the complex does not come into contact with the PEG surface. In the Ab immobilization approach, the antibody forms specific interactions with the protein. Despite the very different interactions present in the immobilization approaches, the same static and dynamic heterogeneity is observed using both techniques. It is unlikely

[20] For fluorescence studies, however, we did see an increase in noise and aberrant fluorophore behaviour (as expected) when the fluorophore stabilising factors were removed.

that both immobilization techniques would cause the exact same heterogeneity; therefore we suggest it is more likely that the observed heterogeneity is an inherent feature of RNAP, at least, in an *in vitro* setting. Future studies are needed to test whether similar heterogeneity is observed *in vivo*.

In addition to investigating the cause of the heterogeneity, it will be of considerable interest to perform statistical analyses of our time trajectory data to quantitatively characterise the observed heterogeneity. Specifically, it will be intriguing to statistically test whether our dynamic molecules conform to a single dynamic population with well-defined kinetic parameters or not. Likelihood ratio tests using the outputs from individual HMM fits could be used to determine if molecules are actually behaving differently (205). This type of analysis could also provide insight into whether the observed static molecules truly conform to an independent population. Current work is addressing these questions.

We investigated the mechanism of initial RNA synthesis using our smFRET assay. Our results showed abortive cycling directly for the first time, which enabled us to characterise the lifetime of the elusive scrunched complexes. We investigated the role of the σR3.2 finger in abortive initiation, and demonstrated that this structural element stabilises short RNAs at the active site and acts as a barrier to the synthesis of long (>5-mer) RNAs. Our smFRET assay was sufficiently sensitive for us to extend our investigations to promoter escape and address a number of open questions regarding the mechanism of escape. Our results suggest that abortive cycling is not an obligatory process for promoter escape, and that in most cases RNAP performs few (0–2) detectable abortive cycles before escaping the *lac* consensus promoter. Future biochemical studies investigating the distribution of RNA products at our promoter under promoter escape conditions will enable us to test our hypothesis regarding the distribution of abortive and productive behaviours. Furthermore, our results suggest that there is some plasticity regarding the exact position at which promoter escape occurs. Our results also reveal an intriguing subpopulation of molecules that are unable to escape the promoter and may correspond to moribund complexes previously reported in the literature (100, 102).

In our final set of experiments, we investigated the conformational dynamics of the RNAP β' clamp. Our results confirm a number of hypotheses put forward in a previous single-molecule study of the clamp conformation (27). In addition we make a number of novel observations. We showed for the first time that the clamp in holoenzyme is able to undergo dynamic fluctuations between open and closed conformations, and our results support a model in which transcription bubble melting occurs after double-stranded DNA has inserted inside the DNA binding cleft. Finally, our results showed that different inhibitors function by locking the clamp in an open or closed conformation. This highlights the functional importance of clamp conformational changes in transcription.

8.1 Future work

The immobilization techniques demonstrated in this thesis have enabled us to make major advances in our efforts to uncover new information regarding the transcription initiation mechanism using single-molecule techniques. Our work raises a number of intriguing questions that we intend to investigate further in the future.

A major goal is to uncover the exact role played by heterogeneity observed throughout this thesis. We are particularly interested in investigating whether the heterogeneity observed in the RNA synthesis reaction has a regulatory function. The Kapanidis group is currently testing a number of potential regulatory molecules that may influence the behaviour of RNAP during initial transcription. There are also plans to investigate what role the promoter sequence and the initial transcribed sequence may play in RNAP pausing during initial RNA synthesis. Pausing is known to play an important regulatory role in elongation (131), and it will be particularly interesting to test whether pausing in initiation also has some regulatory function. Future experiments will involve experiments exploring what effect regulatory proteins such as GreA and GreB have on our abortive initiation and promoter escape assays.

Future work will also investigate whether the behaviours observed at the *lac* consensus promoter in abortive initiation and promoter escape – such as the position at which escape occurs and the number of abortive cycles that precede promoter escape – are unique to this promoter or common features of numerous promoters. We are currently investigating the abortive initiation and promoter escape behaviours of T5 *N25*, T7 *A1*, and *rrnB* P1 promoters.

We are interested in investigating further the transcription bubble dynamics observed in chapter 5. We hypothesized that the bubble dynamics plays a functional role in transcription initiation and intend to test this hypothesis in future studies. We will investigate whether other promoters such as the *rrnB* P1 promoter show similar bubble opening and closing transitions. We will also test whether the subpopulations of complexes exhibiting closed, partially open, open, and dynamic transcription bubbles exhibit different tendencies to perform *de novo* RNA synthesis. This will require the deconvolution of the FRET signals due to transcription bubble dynamics and abortive initiation dynamics. We also hope to use our transcription bubble smFRET assay to investigate which stages of the open complex (RP_O) formation pathway are targeted by inhibitors and regulatory molecules. These studies will complement future investigations looking at the effect of inhibitors and regulatory molecules on the clamp conformation. We are currently investigating the effect of ppGpp and DksA on transcription bubble opening, and the clamp conformation.

In chapter 7, we demonstrated our ability to monitor the clamp conformation at different stages of transcription in real-time. Future investigations will extend this work to investigate the clamp conformation during elongation and termination. We are specifically interested in testing whether clamp opening accompanies RNAP pausing and backtracking during elongation, and uncovering what clamp conformational changes occur during termination.

We anticipate that many of the future investigations outlined above will utilise the vesicle and antibody immobilization strategies demonstrated in chapter 4. We hope that these immobilization approaches will also be used to investigate the transcription mechanisms of archaeal and eukaryotic RNA polymerases. It will be particularly

interesting to see whether the heterogeneity and mechanistic details of initial transcription reported in this thesis, are also features of the archaeal and eukaryotic transcription mechanisms.

Finally, we note that other members of the Kapanidis group have been successful in internalising fluorescently-labelled promoter DNA fragments into live bacterial cells and observing FRET signals that may indicate the formation of active transcription complexes. This raises the exciting possibility of performing experiments with the level of detail demonstrated in this thesis, inside of live bacterial cells.

Appendix A: *E. coli* RNAP-promoter DNA complex structural model

A.1 RP_O model

Throughout this thesis we use a structural model of *E. coli* RP_O to make structural predictions and measure distances. The *Thermus aquaticus* RP_O model from (49) was used as the basis for our *E. coli* RP_O model. We combined the following elements in our model:

- Protein from *E. coli* holoenzyme (PDB 4IGC) (16);
- DNA from the *T. aquaticus* RP_O model [-60 to -5, nontemplate strand; -60 to -13, template strand; +13 to +21 of both strands (49)];
- DNA from the *T. thermophilus* RNAP-fork junction DNA structure [-4 to +12 template strand; -12 to +12 nontemplate strand (PDB 4G7H) (72)];
- B-form DNA (+22 to +35)

Our model was created by first performing a structural alignment between the *T. aquaticus* RP_O model and the *E. coli* holoenzyme structure. The resulting intermediate model (I1) was then structurally aligned with the *T. thermophilus* RNAP-fork junction DNA structure to form an intermediate model (I2). Finally, B-form DNA was generated using 3D-DART (206) and overlapping bases aligned onto the +21 end of our intermediate model to generate our final *E. coli* RP_O model (Fig. A1A). We justify our structural alignment approach in creating an *E.* coli RP_O model based on the following observations: 1) Sequence identity between *E. coli* and *T. aquaticus* and between *E. coli* and *T. thermophilus* is high at ~30%, and 2) the *E. coli* RNAP structure is highly similar to both the *T. aquaticus* and *T. thermophilus* RNAP structures (16) with root-mean-square-deviation (RMSD) values for atom deviations of 2.7 Å (*E. coli* & *T. aquaticus*) and 2.3 Å (*E. coli* & *T. thermophilus*).

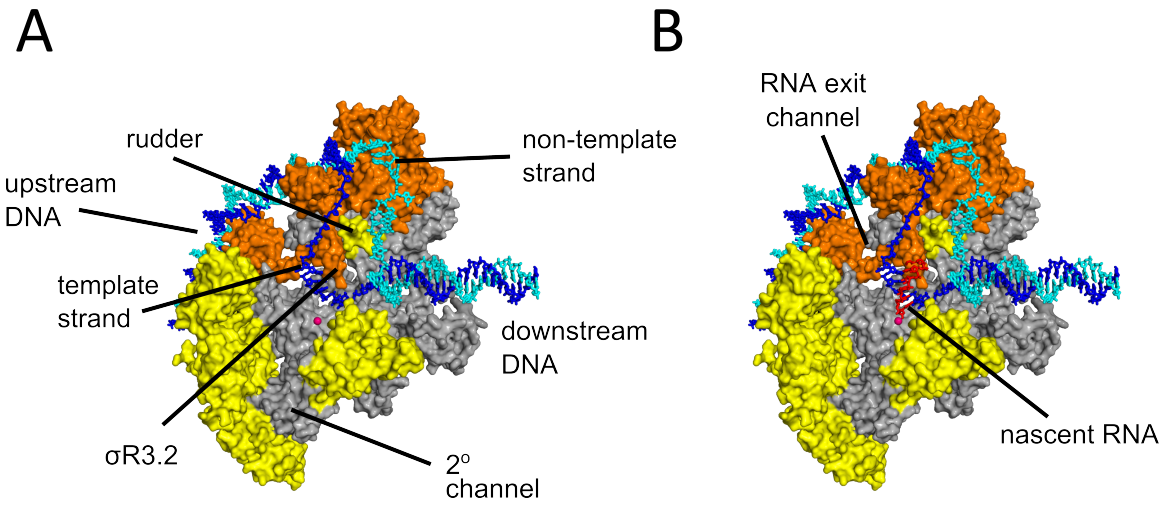


Figure A1. *E. coli* RNAP-promoter DNA complex structural models. (A) Cut-away structural model of *E. coli* RP_O. Major structural regions are highlighted. σ^{70} is shown in orange and core protein is shown in grey except for the regions that protrude in front of the cut-away plane, which are yellow. The β subunit and σR1.1 are omitted for clarity. The template strand is shown in dark blue; the non-template strand in light blue. Downstream DNA ends at +25 in the figure. (B) Cut-away structural model of *E. coli* RP_{ITC6}. Scrunched DNA is not shown. Images were created using Pymol.

A.2 RP_{ITC} models

In this section we describe how we generated RP_{ITC} structural models used to determine what length nascent RNAs need to be to clash with the σR3.2 finger in chapter 6.

We performed a structural alignment between our *E. coli* RP_O model (section A.1) and the *T. thermophilus* RNAP elongation complex (PDB 2O5I) (25) in order to incorporate the RNA chain atoms from the elongation complex into our RP_O model. We modelled RP_{ITC3}, RP_{ITC4}, RP_{ITC5}, and RP_{ITC6} by limiting the length of the RNA at the active site to 3-, 4-, 5-, and 6-nt. Despite the high structural similarity between the *E. coli*, *T. aquaticus*, and *T. thermophilus* RNAP structures, we observed small differences at the active site that altered the length the nascent RNA needed to be to clash with the σR3.2 finger. This variation was due to different lengths of the σR3.2 loop in the three structures; we therefore used the *E. coli* structural model when interpreting the *E. coli* smFRET results presented in chapter 6.

A.3 RNAP His-tag location

In the majority of experiments performed in this thesis, we immobilize RNAP using a penta-His antibody. Here, surface-immobilized antibody anchors RNAP molecules to the surface by binding to the RNAP His-tag. The location of the His-tag on the *E. coli* RP_O structure is shown in Fig. A2.

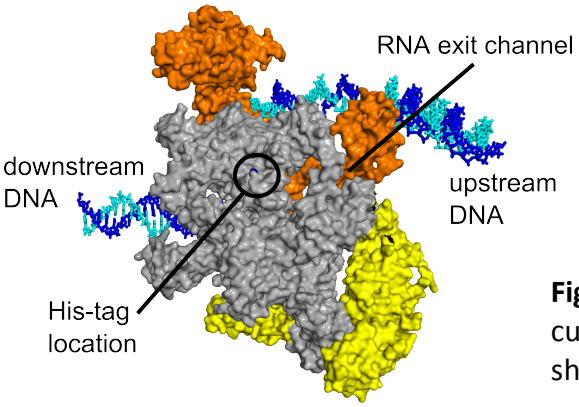


Figure A2. Location of RNAP His-tag. Same cut-away structural model of *E. coli* RP_O shown in Fig. A1A viewed from behind.

Appendix B: Additional real-time RNA synthesis results

B.1 Leading edge-FRET (LE-FRET) shows similar heterogeneity in abortive initiation

In chapter 6 we demonstrated our ability to monitor initial RNA synthesis using a smFRET assay in which the donor dye was attached to the promoter DNA at position -15 and the acceptor dye attached to position +20, relative to the transcription start site (+1). To observe initial RNA synthesis using a different vantage point, we performed smFRET TIRF microscopy experiments using a LE-FRET assay. In these experiments, we used a σ^{70} subunit labelled at position 366 with the donor dye, Cy3B. The fluorescently labelled σ^{70} subunit was a gift from Dr. Richard Ebright (Rutgers University, USA), and has been used to monitor abortive initiation in a previous study (6). Fig. B1 shows a schematic of the expected fluorophore movements using this LE-FRET assay.

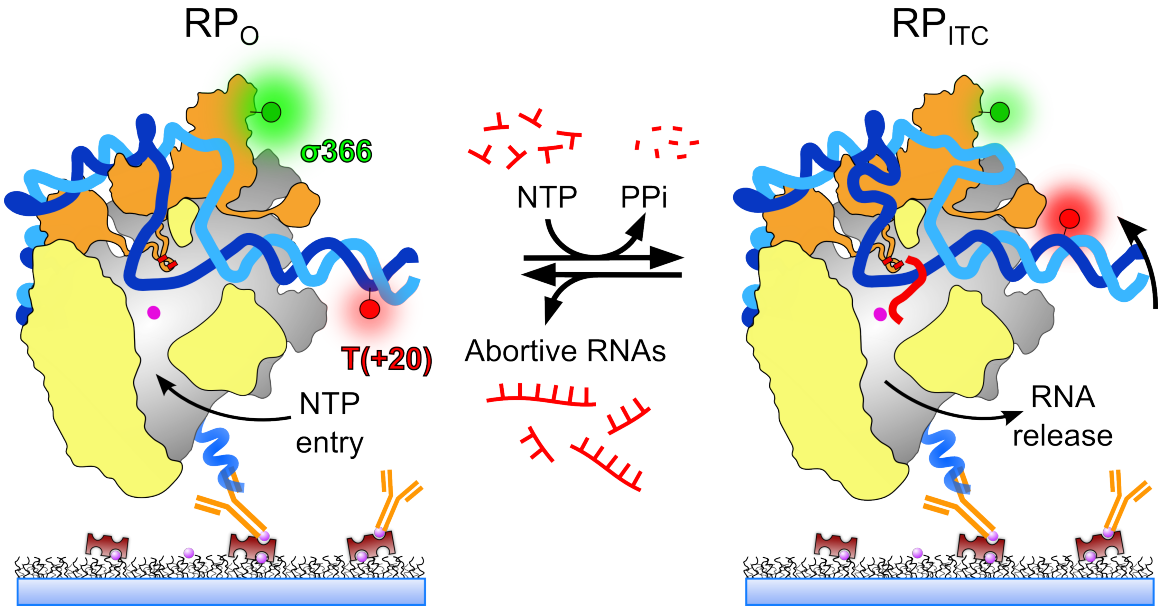


Figure B1. Schematic of LE-FRET assay. The penta-His antibody binds to the RNAP His-tag and anchors the RNAP to the surface (see chapter 5). The donor and acceptor dyes are labelled and shown in green and red, respectively. RNA is shown as a red strand at the active site in RPITC. The movement of the acceptor dye is shown with an arrow. RNAP and the promoter DNA are coloured as in *Appendix A*.

We performed $RP_{ITC\leq7}$ experiments as described in chapter 6. In these LE-FRET experiments we used a lacCONS+2 promoter DNA fragment labelled only with an acceptor dye at the +20 position. The DNA fragment was not labelled with a donor dye (Fig. B2). Our results showed the same qualitative behaviour and heterogeneity as described in chapter 6. Two example traces of a stably scrunched molecule and an abortive cycling molecule can be seen in Fig. B3. Based on these observations we concluded that the donor dye attachment position has no influence on the behaviour of RNAP in abortive initiation. It should be noted that when the donor dye, Cy3B, was attached to σ^{70} it appeared to bleach more rapidly and was less bright than when attached to the promoter DNA. Presumably this was due to changes in the local environment of the fluorophore.

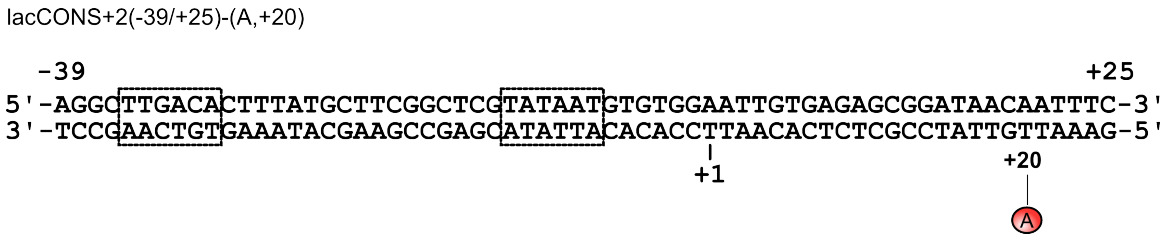


Figure B2. Promoter DNA fragment used for LE-FRET experiments. Promoter DNA fragment labelled with ATTO647N. The black boxes indicate the -10 and -35 elements. The transcription start site is labelled, as is the fluorophore labelling site.

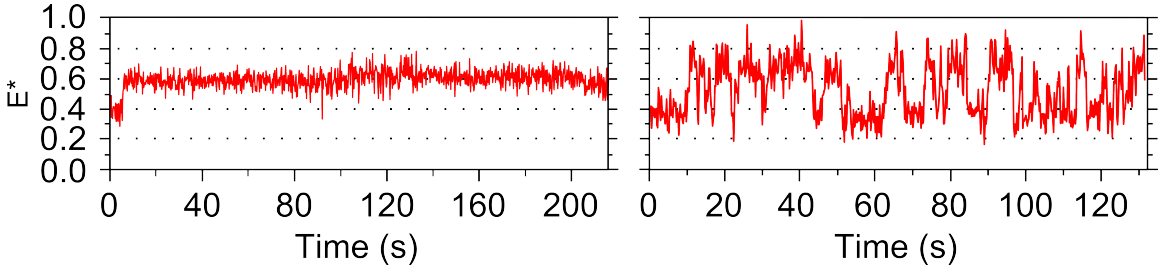


Figure B3. Abortive initiation observed using a LE-FRET assay. Example time trajectories of transcribing complexes ($RP_{ITC\leq7}$ conditions) displaying stable scrunched behaviour (left), and cycling behaviour (right). Temporal resolution is 200 ms.

B.2 Actively transcribing complexes occasionally exhibit switching behaviour

Experiments in which we monitored the abortive cycling behaviour of RNAP molecules revealed rare instances (<1% of actively transcribing complexes) where molecules appeared to display changes in behaviour during our observation period. Fig. B4 shows example time trajectories of molecules displaying this behaviour. It is tempting to speculate that differences in conformational states in the polymerase or promoter DNA lead to these changes in behaviour. However, further experiments are necessary to determine whether this hypothesis is correct. In the future we hope to extend our observation periods well beyond what we currently achieve (~300 sec) in order to observe more example of switching behaviour.

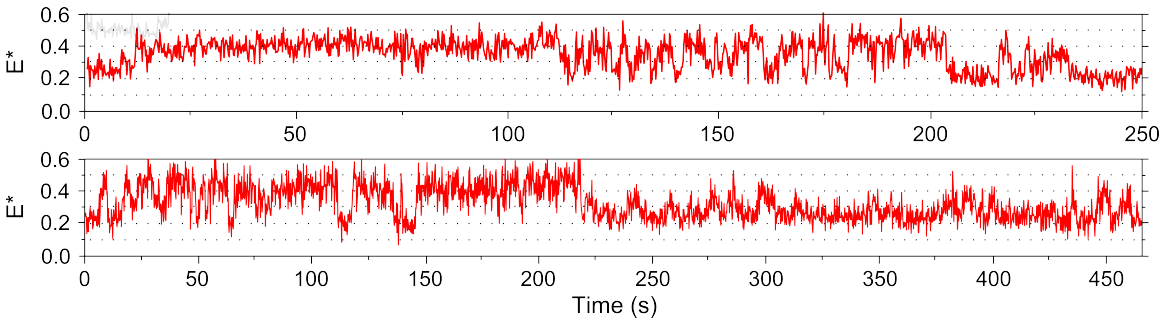


Figure B4. Switching behaviour. Example time trajectories of transcribing complexes ($RP_{ITC\leq7}$ conditions) displaying changes in behaviour. Temporal resolution is 200 ms.

Appendix C: Additional dwell time distributions

C.1 RP_O bubble dynamics

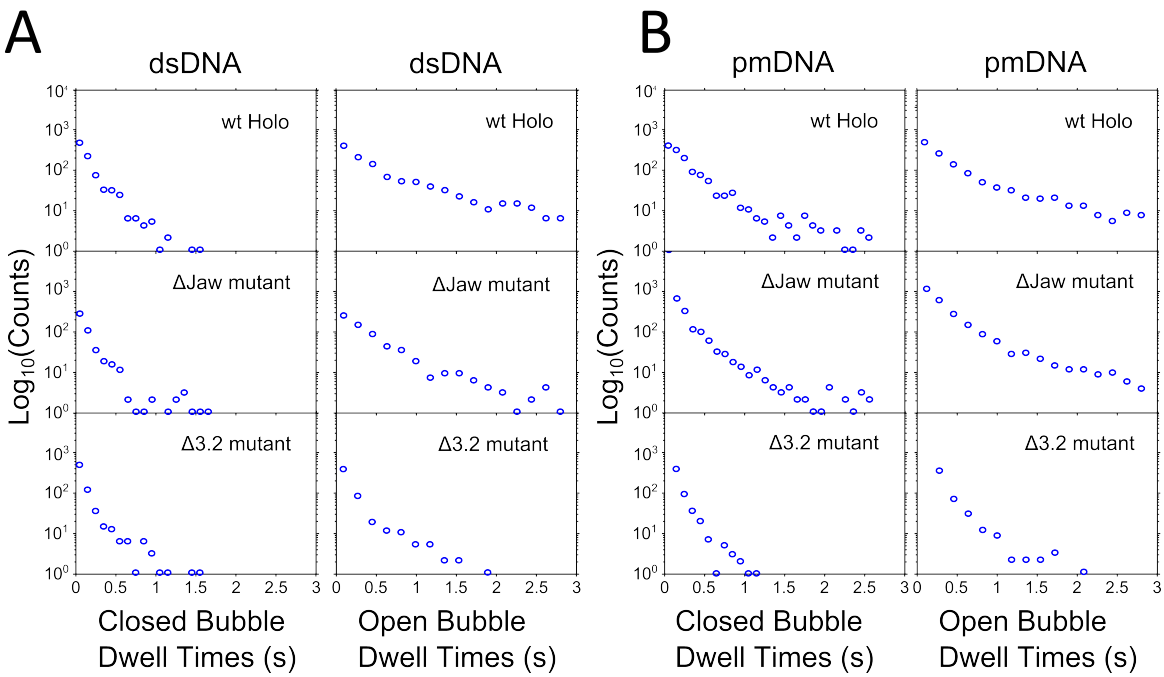


Figure C1. Kinetics of transcription bubble dynamics: extended. This figure shows the same data as in Fig. 5.15D–E except here the counts axis is plotted on a logarithmic scale. (A) Stacked plots of closed and open bubble conformation dwells for dsDNA. 852 events from 80 molecules are shown in the top panels, 692 events from 71 molecules are shown in the middle panels, 924 events from 85 molecules are shown in the bottom panels. (B) Stacked histograms of closed and open bubble conformation dwells for pmDNA. For figures A and B, wt data is shown in the top panel, ΔJaw mutant data in the middle panel, Δ 3.2 mutant data in the bottom panel. 1165 events from 87 molecules are shown in the top panels, 2001 events from 101 molecules are shown in the middle panels, 2082 events from 105 molecules are shown in the bottom panels. Temporal resolution is 20 ms.

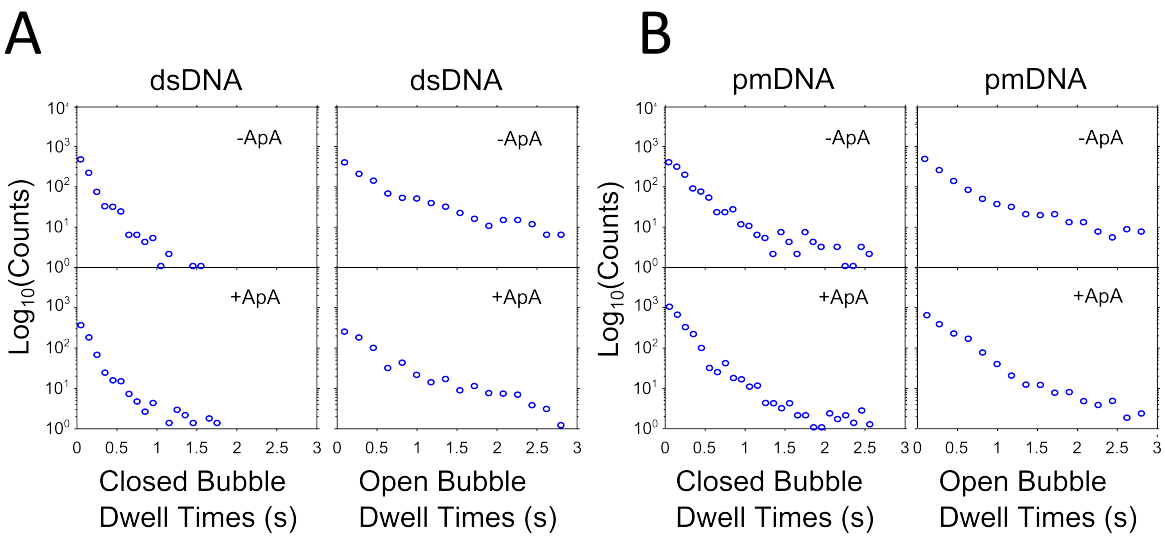


Figure C2. ApA effect on kinetics of transcription bubble dynamics: extended. This figure shows the same data as in Fig. 5.16 except here the counts axis is plotted on a logarithmic scale. (A) Stacked plots of closed and open bubble conformation dwells for dsDNA. 852 events from 80 molecules are shown in the top panels, 793 events from 78 molecules are shown in the bottom panels. (B) Stacked histograms of closed and open bubble conformation dwells for pmDNA. For figures A and B, wt data is shown in the top panel, ΔJaw mutant data in the middle panel, Δ 3.2 mutant data in the bottom panel. 1165 events from 87 molecules are shown in the top panels, 1111 events from 94 molecules are shown in the bottom panels. Temporal resolution is 20 ms.

C.2 Abortive cycling dynamics

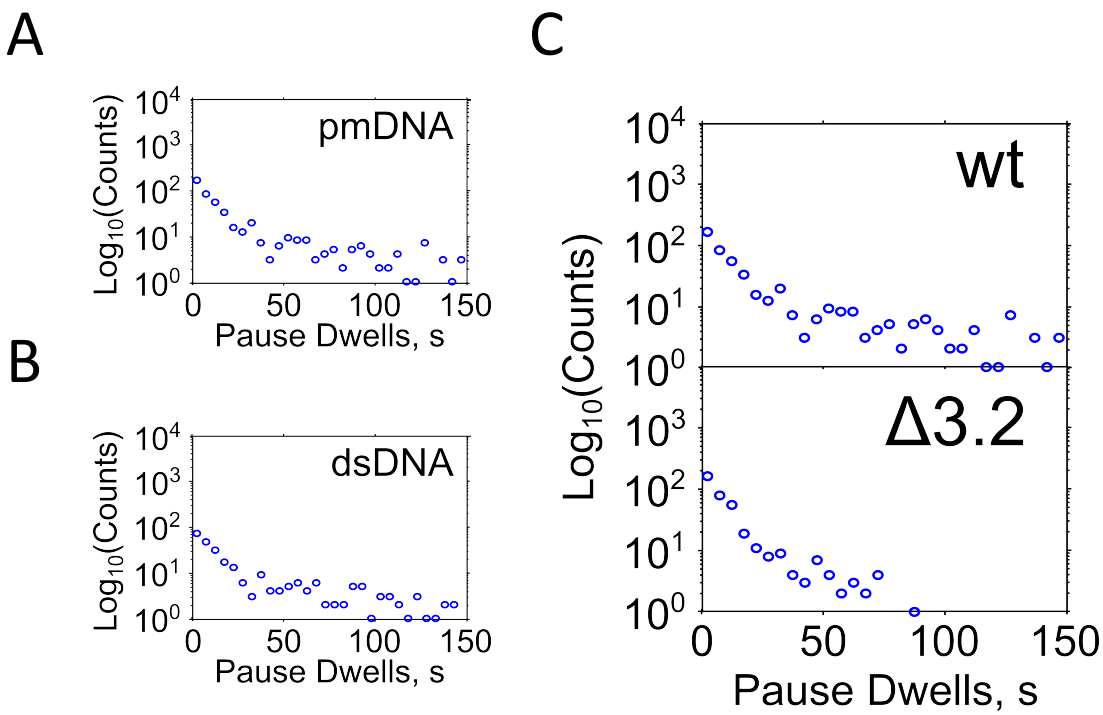


Figure C3. Scrunched state dwell times: extended. This figure shows the same dwell time data as in chapter 6 except here the counts axis is plotted on a logarithmic scale. (A) Shows data from the dwell time histogram in Fig. 6.10 and corresponds to scrunched state dwell times for initiation complexes formed using pre-melted DNA. The plot shows 445 events from 112 molecules. (B) Shows data from the dwell time histogram in Fig. 6.11 and corresponds to scrunched state dwell times for initiation complexes formed using fully complementary dsDNA. The plot shows 250 events from 91 molecules. (C) Shows data from the dwell time histograms in Fig. 6.13. The top histogram shows wt holoenzyme data (445 events from 112 molecules) while the bottom histogram shows Δ3.2 mutant data (392 events from 95 molecules). Temporal resolution is 20 ms.

Bibliography

1. Michaelis J, Treutlein B (2013) Single-molecule studies of RNA polymerases. *Chem Rev* 113:8377–99.

2. Abbondanzieri EA, Greenleaf WJ, Shaevitz JW, Landick R, Block SM (2005) Direct observation of base-pair stepping by RNA polymerase. *Nature* 438:460–5.

3. Forde NR, Izhaky D, Woodcock GR, Wuite GJL, Bustamante C (2002) Using mechanical force to probe the mechanism of pausing and arrest during continuous elongation by Escherichia coli RNA polymerase. *Proc Natl Acad Sci U S A* 99:11682–7.

4. Andrecka J et al. (2008) Single-molecule tracking of mRNA exiting from RNA polymerase II. *Proc Natl Acad Sci U S A* 105:135–40.

5. Andrecka J et al. (2009) Nano positioning system reveals the course of upstream and nontemplate DNA within the RNA polymerase II elongation complex. *Nucleic Acids Res* 37:5803–9.

6. Kapanidis AN et al. (2006) Initial transcription by RNA polymerase proceeds through a DNA-scrunching mechanism. *Science* 314:1144–7.

7. Revyakin A, Liu C, Ebright RH, Strick TR (2006) Abortive initiation and productive initiation by RNA polymerase involve DNA scrunching. *Science* 314:1139–43.

8. Friedman LJ, Gelles J (2012) Mechanism of transcription initiation at an activator-dependent promoter defined by single-molecule observation. *Cell* 148:679–89.

9. Jacob F, Monod J (1961) On the Regulation of Gene Activity. *Cold Spring Harb Symp Quant Biol* 26:193–211.

10. Busby S, Kolb A, Buc H (2009) in *RNA Polymerases as Molecular Motors*, eds Buc H, Strick T (Royal Society of Chemistry, Cambridge), pp 13–37.

11. Chamberlin M, Berg P (1962) Deoxyribo ucleic acid-directed synthesis of ribonucleic acid by an enzyme from Escherichia coli. *Proc Natl Acad Sci U S A* 48:81–94.

12. Furth J., Hurwitz J, Anders M (1962) The Role of Deoxyribonucleic Acid in Ribonucleic Acid Synthesis: I. The Purification and Properties of Ribonucleic Acid Polymerase. *J Biol Chem* 237:2611–2619.

13. Hurwitz J, Furth JJ, Anders M, Ortiz PJ, August JT (1961) The Enzymatic Incorporation of Ribonucleotides into RNA and the Role of DNA. *Cold Spring Harb Symp Quant Biol* 26:91–100.

14. Werner F, Grohmann D (2011) Evolution of multisubunit RNA polymerases in the three domains of life. *Nat Rev Microbiol* 9:85–98.

15. Ebright RH, Busby S (1995) The Escherichia coli RNA polymerase alpha subunit: structure and function. *Curr Opin Genet Dev* 5:197–203.

16. Murakami KS (2013) X-ray crystal structure of Escherichia coli RNA polymerase σ70 holoenzyme. *J Biol Chem* 288:9126–34.

17. Murakami KS, Masuda S, Darst SA (2002) Structural basis of transcription initiation: RNA polymerase holoenzyme at 4 A resolution. *Science* 296:1280–4.

18. Vassylyev DG et al. (2002) Crystal structure of a bacterial RNA polymerase holoenzyme at 2.6 A resolution. *Nature* 417:712–9.

19. Gezvain K., Landick R (2004) in *The bacterial chromosome*, ed Higgins N. (American Society for Microbiology, Washington, DC), pp 283–296.

20. Ghosh P, Ishihama A, Chatterji D (2001) Escherichia coli RNA polymerase subunit omega and its N-terminal domain bind full-length beta' to facilitate incorporation into the alpha2beta subassembly. *Eur J Biochem* 268:4621–7.

21. Tang H, Severinov K, Goldfarb A, Ebright RH (1995) Rapid RNA polymerase genetics: one-day, no-column preparation of reconstituted recombinant Escherichia coli RNA polymerase. *Proc Natl Acad Sci U S A* 92:4902–6.

22. Campbell EA et al. (2001) Structural mechanism for rifampicin inhibition of bacterial rna polymerase. *Cell* 104:901–12.

23. Weixlbaumer A, Leon K, Landick R, Darst SA (2013) Structural basis of transcriptional pausing in bacteria. *Cell* 152:431–41.

24. Tagami S et al. (2010) Crystal structure of bacterial RNA polymerase bound with a transcription inhibitor protein. *Nature* 468:978–82.

25. Vassylyev DG, Vassylyeva MN, Perederina A, Tahirov TH, Artsimovitch I (2007) Structural basis for transcription elongation by bacterial RNA polymerase. *Nature* 448:157–62.

26. Basu RS et al. (2014) Structural Basis of Transcription Initiation by Bacterial RNA Polymerase holoenzyme. *J Biol Chem*:M114.584037–.

27. Chakraborty A et al. (2012) Opening and closing of the bacterial RNA polymerase clamp. *Science* 337:591–5.

28. Nayak D, Voss M, Windgassen T, Mooney RA, Landick R (2013) Cys-pair reporters detect a constrained trigger loop in a paused RNA polymerase. *Mol Cell* 50:882–93.

29. Erie DA, Kennedy SR (2009) Forks, pincers, and triggers: the tools for nucleotide incorporation and translocation in multi-subunit RNA polymerases. *Curr Opin Struct Biol* 19:708–14.

30. Vassylyev DG et al. (2007) Structural basis for substrate loading in bacterial RNA polymerase. *Nature* 448:163–8.

31. Steitz TA (1998) A mechanism for all polymerases. *Nature* 391:231–2.

32. Sosunov V et al. (2003) Unified two-metal mechanism of RNA synthesis and degradation by RNA polymerase. *EMBO J* 22:2234–44.

33. Borukhov S, Sagitov V, Goldfarb A (1993) Transcript cleavage factors from E. coli. *Cell* 72:459–466.

34. Zenkin N, Yuzenkova Y, Severinov K (2006) Transcript-assisted transcriptional proofreading. *Science* 313:518–20.

35. Landick R (2005) NTP-entry routes in multi-subunit RNA polymerases. *Trends Biochem Sci* 30:651–4.

36. Nickels BE, Hochschild A (2004) Regulation of RNA polymerase through the secondary channel. *Cell* 118:281–4.

37. Opalka N et al. (2003) Structure and function of the transcription elongation factor GreB bound to bacterial RNA polymerase. *Cell* 114:335–45.

38. Cramer P (2002) Multisubunit RNA polymerases. *Curr Opin Struct Biol* 12:89–97.

39. Yakhnin A V, Babitzke P (2014) NusG/Spt5: are there common functions of this ubiquitous transcription elongation factor? *Curr Opin Microbiol* 18C:68–71.

40. Mekler V, Minakhin L, Severinov K (2011) A critical role of downstream RNA polymerase-promoter interactions in the formation of initiation complex. *J Biol Chem* 286:22600–8.

41. Drennan A et al. (2012) Key Roles of the Downstream Mobile Jaw of Escherichia coli RNA Polymerase in Transcription Initiation. *Biochemistry*.

42. Zhang J, Landick R (2009) in *RNA Polymerases as Molecular Motors*, eds Buc H, Strick T (Royal Society of Chemistry), pp 206–235.

43. Decker KB, Hinton DM (2013) Transcription regulation at the core: similarities among bacterial, archaeal, and eukaryotic RNA polymerases. *Annu Rev Microbiol* 67:113–39.

44. Harley CB, Reynolds RP (1987) Analysis of E. coli promoter sequences. *Nucleic Acids Res* 15:2343–61.

45. Hawley DK, McClure WR (1983) Compilation and analysis of Escherichia coli promoter DNA sequences. *Nucleic Acids Res* 11:2237–2255.

46. McClure WR (1985) Mechanism and control of transcription initiation in prokaryotes. *Annu Rev Biochem* 54:171–204.

47. Haugen SP, Ross W, Gourse RL (2008) Advances in bacterial promoter recognition and its control by factors that do not bind DNA. *Nat Rev Microbiol* 6:507–19.

48. Beutel BA, Record MT (1990) E. coli promoter spacer regions contain nonrandom sequences which correlate to spacer length. *Nucleic Acids Res* 18:3597–603.

49. Murakami KS, Masuda S, Campbell EA, Muzzin O, Darst SA (2002) Structural basis of transcription initiation: an RNA polymerase holoenzyme-DNA complex. *Science* 296:1285–90.

50. Ross W et al. (1993) A third recognition element in bacterial promoters: DNA binding by the alpha subunit of RNA polymerase. *Science* 262:1407–13.

51. Tagami H, Aiba H (1999) An inactive open complex mediated by an UP element at Escherichia coli promoters. *Proc Natl Acad Sci* 96:7202–7207.

52. Burgess RR, Travers AA, Dunn JJ, Bautz EK (1969) Factor stimulating transcription by RNA polymerase. *Nature* 221:43–6.

53. Travers AA, Burgessrr (1969) Cyclic re-use of the RNA polymerase sigma factor. *Nature* 222:537–40.

54. Murakami KS, Darst SA (2003) Bacterial RNA polymerases: the wholo story. *Curr Opin Struct Biol* 13:31–9.

55. Borukhov S, Severinov K (2002) Role of the RNA polymerase sigma subunit in transcription initiation. *Res Microbiol* 153:557–62.

56. Busby S, Ebright RH (1994) Promoter structure, promoter recognition, and transcription activation in prokaryotes. *Cell* 79:743–6.

57. Helmann JD, Chamberlin MJ (1988) Structure and function of bacterial sigma factors. *Annu Rev Biochem* 57:839–72.

58. Paget MSB, Helmann JD (2003) The sigma70 family of sigma factors. *Genome Biol* 4:203.

59. Campbell EA et al. (2002) Structure of the bacterial RNA polymerase promoter specificity sigma subunit. *Mol Cell* 9:527–39.

60. Pupov D, Kuzin I, Bass I, Kulbachinskiy A (2014) Distinct functions of the RNA polymerase σ subunit region 3.2 in RNA priming and promoter escape. *Nucleic Acids Res*.

61. Mekler V et al. (2002) Structural Organization of Bacterial RNA Polymerase Holoenzyme and the RNA Polymerase-Promoter Open Complex. *Cell* 108:599–614.

62. Vassylyev DG et al. (2002) Crystal structure of a bacterial RNA polymerase holoenzyme at 2.6 A resolution. *Nature* 417:712–9.

63. Davis CA, Bingman CA, Landick R, Record MT, Saecker RM (2007) Real-time footprinting of DNA in the first kinetically significant intermediate in open complex formation by Escherichia coli RNA polymerase. *Proc Natl Acad Sci U S A* 104:7833–8.

64. Gries TJ, Kontur WS, Capp MW, Saecker RM, Record MT (2010) One-step DNA melting in the RNA polymerase cleft opens the initiation bubble to form an unstable open complex. *Proc Natl Acad Sci U S A* 107:10418–23.

65. Buc H, McClure WR (1985) Kinetics of open complex formation between Escherichia coli RNA polymerase and the lac UV5 promoter. Evidence for a sequential mechanism involving three steps. *Biochemistry* 24:2712–23.

66. Saecker RM, Record MT, Dehaseth PL (2011) Mechanism of bacterial transcription initiation: RNA polymerase - promoter binding, isomerization to initiation-competent open complexes, and initiation of RNA synthesis. *J Mol Biol* 412:754–71.

67. Studitsky V, Brodolin K, Liu Y, Mirzabekov A (2001) Topography of lacUV5 initiation complexes. *Nucleic Acids Res* 29:854–61.

68. Brodolin K (2011) Antibiotics trapping transcription initiation intermediates: To melt or to bend, what's first? *Transcription* 2:60–65.

69. Helmann JD, DeHaseth PL (1999) Protein-nucleic acid interactions during open complex formation investigated by systematic alteration of the protein and DNA binding partners. *Biochemistry* 38:5959–67.

70. Juang YL, Helmann JD (1994) A promoter melting region in the primary sigma factor of Bacillus subtilis. Identification of functionally important aromatic amino acids. *J Mol Biol* 235:1470–88.

71. Shultzaberger RK, Chen Z, Lewis KA, Schneider TD (2007) Anatomy of Escherichia coli sigma70 promoters. *Nucleic Acids Res* 35:771–88.

72. Zhang Y et al. (2012) Structural basis of transcription initiation. *Science* 338:1076–80.

73. Feklistov A, Darst SA (2011) Structural basis for promoter-10 element recognition by the bacterial RNA polymerase σ subunit. *Cell* 147:1257–69.

74. Rogozina A, Zaychikov E, Buckle M, Heumann H, Sclavi B (2009) DNA melting by RNA polymerase at the T7A1 promoter precedes the rate-limiting step at 37 degrees C and results in the accumulation of an off-pathway intermediate. *Nucleic Acids Res* 37:5390–404.

75. Saecker RM et al. (2002) Kinetic studies and structural models of the association of E. coli sigma(70) RNA polymerase with the lambdaP(R) promoter: large scale conformational changes in forming the kinetically significant intermediates. *J Mol Biol* 319:649–71.

76. Craig ML et al. (1998) DNA footprints of the two kinetically significant intermediates in formation of an RNA polymerase-promoter open complex: evidence that interactions with start site and downstream DNA induce sequential conformational changes in polymerase and DNA. *J Mol Biol* 283:741–56.

77. Spassky A, Kirkegaard K, Buc H (1985) Changes in the DNA structure of the lac UV5 promoter during formation of an open complex with Escherichia coli RNA polymerase. *Biochemistry* 24:2723–31.

78. Kontur WS, Capp MW, Gries TJ, Saecker RM, Record MT (2010) Probing DNA binding, DNA opening, and assembly of a downstream clamp/jaw in Escherichia coli RNA polymerase-lambdaP(R) promoter complexes using salt and the physiological anion glutamate. *Biochemistry* 49:4361–73.

79. Chen J, Darst SA, Thirumalai D (2010) Promoter melting triggered by bacterial RNA polymerase occurs in three steps. *Proc Natl Acad Sci U S A* 107:12523–8.

80. Tupin A, Gualtieri M, Leonetti J-P, Brodolin K (2010) The transcription inhibitor lipiarmycin blocks DNA fitting into the RNA polymerase catalytic site. *EMBO J* 29:2527–37.

81. Carpousis AJ, Gralla JD (1980) Cycling of ribonucleic acid polymerase to produce oligonucleotides during initiation in vitro at the lac UV5 promoter. *Biochemistry* 19:3245–3253.

82. Johnston DE, McClure WR (1976) in *RNA Polymerase*, eds Losick R, Chamberlin MJ (Cold Spring Harbor Laboratory Press, New York), pp 413–428.

83. Chander M, Austin KM, Aye-Han N-N, Sircar P, Hsu LM (2007) An alternate mechanism of abortive release marked by the formation of very long abortive transcripts. *Biochemistry* 46:12687–99.

84. Hsu LM (2009) Monitoring abortive initiation. *Methods* 47:25–36.

85. Hsu LM, Vo N V., Chamberlin MJ (1995) Escherichia coli transcript cleavage factors GreA and GreB stimulate promoter escape and gene expression in vivo and in vitro. *Proc Natl Acad Sci* 92:11588–11592.

86. Feng G, Lee D, Wang D, Chan C, Landick R (1994) GreA-induced transcript cleavage in transcription complexes containing Escherichia coli RNA polymerase is controlled by multiple factors, including nascent transcript location and structure. *J Biol Chem* 269:22282–22294.

87. Stepanova E et al. (2007) Analysis of promoter targets for Escherichia coli transcription elongation factor GreA in vivo and in vitro. *J Bacteriol* 189:8772–85.

88. Hsu LM et al. (2006) Initial transcribed sequence mutations specifically affect promoter escape properties. *Biochemistry* 45:8841–54.

89. Werner F, Weinzierl ROJ (2005) Direct modulation of RNA polymerase core functions by basal transcription factors. *Mol Cell Biol* 25:8344–55.

90. Luse DS, Jacob GA (1987) Abortive initiation by RNA polymerase II in vitro at the adenovirus 2 major late promoter. *J Biol Chem* 262:14990–14997.

91. Goldman SR, Ebright RH, Nickels BE (2009) Direct detection of abortive RNA transcripts in vivo. *Science* 324:927–8.

92. Hsu LM, Vo N V, Kane CM, Chamberlin MJ (2003) In vitro studies of transcript initiation by Escherichia coli RNA polymerase. 1. RNA chain initiation, abortive initiation, and promoter escape at three bacteriophage promoters. *Biochemistry* 42:3777–86.

93. Hawley DK, McClure WR (1980) In vitro comparison of initiation properties of bacteriophage lambda wild-type PR and x3 mutant promoters. *Proc Natl Acad Sci U S A* 77:6381–5.

94. Brunner M, Bujard H (1987) Promoter recognition and promoter strength in the Escherichia coli system. *EMBO J* 6:3139–44.

95. McClure WR (1985) Mechanism and control of transcription initiation in prokaryotes. *Annu Rev Biochem* 54:171–204.

96. Carpousis AJ, Stefano JE, Gralla JD (1982) 5’ Nucleotide heterogeneity and altered initiation of transcription at mutant lac promoters. *J Mol Biol* 157:619–633.

97. Vo N V, Hsu LM, Kane CM, Chamberlin MJ (2003) In vitro studies of transcript initiation by Escherichia coli RNA polymerase. 3. Influences of individual DNA elements within the promoter recognition region on abortive initiation and promoter escape. *Biochemistry* 42:3798–811.

98. Levin JR, Krummel B, Chamberlin MJ (1987) Isolation and properties of transcribing ternary complexes of Escherichia coli RNA polymerase positioned at a single template base. *J Mol Biol* 196:85–100.

99. Gourse RL (1988) Visualization and quantitative analysis of complex formation between E.coli RNA polymerase and an rRNA promoter in vitro. *Nucleic Acids Res* 16:9789–9809.

100. Kubori T, Shimamoto N (1996) A branched pathway in the early stage of transcription by Escherichia coli RNA polymerase. *J Mol Biol* 256:449–57.

101. Sen R (1998) Reduction in Abortive Transcription from the lambda PR Promoter by Mutations in Region 3 of the sigma 70 Subunit of Escherichia coli RNA Polymerase. *J Biol Chem* 273:9872–9877.

102. Susa M, Sen R, Shimamoto N (2002) Generality of the branched pathway in transcription initiation by Escherichia coli RNA polymerase. *J Biol Chem* 277:15407–12.

103. Monsalve M, Mencia M, Rojo F, Salas M (1996) Activation and repression of transcription at two different phage phi29 promoters are mediated by interaction of the same residues of regulatory protein p4 with RNA polymerase. *EMBO J* 15:383–91.

104. Lee J, Goldfarb A (1991) lac repressor acts by modifying the initial transcribing complex so that it cannot leave the promoter. *Cell* 66:793–798.

105. Straney SB, Crothers DM (1987) Lac repressor is a transient gene-activating protein. *Cell* 51:699–707.

106. Menendez M, Kolb A, Buc H (1987) A new target for CRP action at the malT promoter. *EMBO J* 6:4227–34.

107. Sen R, Nagai H, Shimamoto N (2001) Conformational switching of Escherichia coli RNA polymerase-promoter binary complex is facilitated by elongation factor GreA and GreB. *Genes Cells* 6:389–401.

108. Vvedenskaya IO et al. (2012) Growth phase-dependent control of transcription start site selection and gene expression by nanoRNAs. *Genes Dev* 26:1498–507.

109. Hsu LM (2002) Promoter clearance and escape in prokaryotes. *Biochim Biophys Acta* 1577:191–207.

110. Reppas NB, Wade JT, Church GM, Struhl K (2006) The transition between transcriptional initiation and elongation in E. coli is highly variable and often rate limiting. *Mol Cell* 24:747–57.

111. Muse GW et al. (2007) RNA polymerase is poised for activation across the genome. *Nat Genet* 39:1507–11.

112. Zhou Y, Navaroli DM, Enuameh MS, Martin CT (2007) Dissociation of halted T7 RNA polymerase elongation complexes proceeds via a forward-translocation mechanism. *Proc Natl Acad Sci U S A* 104:10352–7.

113. Young BA, Gruber TM, Gross CA (2002) Views of Transcription Initiation. *Cell* 109:417–420.

114. Kapanidis AN et al. (2005) Retention of transcription initiation factor sigma70 in transcription elongation: single-molecule analysis. *Mol Cell* 20:347–56.

115. Marr MT, Datwyler SA, Meares CF, Roberts JW (2001) Restructuring of an RNA polymerase holoenzyme elongation complex by lambdoid phage Q proteins. *Proc Natl Acad Sci U S A* 98:8972–8.

116. Samanta S, Martin CT (2013) Insights into the mechanism of initial transcription in Escherichia coli RNA polymerase. *J Biol Chem* 288:31993–2003.

117. Sainsbury S, Niesser J, Cramer P (2012) Structure and function of the initially transcribing RNA polymerase II–TFIIB complex. *Nature* 493:437–440.

118. Cramer P, Bushnell DA, Kornberg RD (2001) Structural basis of transcription: RNA polymerase II at 2.8 angstrom resolution. *Science* 292:1863–76.

119. Zhang G et al. (1999) Crystal structure of Thermus aquaticus core RNA polymerase at 3.3 A resolution. *Cell* 98:811–24.

120. Gnatt AL, Cramer P, Fu J, Bushnell DA, Kornberg RD (2001) Structural basis of transcription: an RNA polymerase II elongation complex at 3.3 A resolution. *Science* 292:1876–82.

121. Landick R (2001) RNA Polymerase Clamps Down. *Cell* 105:567–570.

122. Belogurov GA et al. (2009) Transcription inactivation through local refolding of the RNA polymerase structure. *Nature* 457:332–5.

123. Mukhopadhyay J et al. (2008) The RNA polymerase “switch region” is a target for inhibitors. *Cell* 135:295–307.

124. Irschik H, Gerth K, Höfle G, Kohl W, Reichenbach H (1983) The myxopyronins, new inhibitors of bacterial RNA synthesis from Myxococcus fulvus (Myxobacterales). *J Antibiot (Tokyo)* 36:1651–8.

125. Srivastava A et al. (2011) New target for inhibition of bacterial RNA polymerase: “switch region”. *Curr Opin Microbiol* 14:532–43.

126. Kurabachew M et al. (2008) Lipiarmycin targets RNA polymerase and has good activity against multidrug-resistant strains of Mycobacterium tuberculosis. *J Antimicrob Chemother* 62:713–9.

127. Coronelli C, White RJ, Lancini GC, Parenti F (1975) Lipiarmycin, a new antibiotic from Actinoplanes. II. Isolation, chemical, biological and biochemical characterization. *J Antibiot (Tokyo)* 28:253–9.

128. Herbert KM, Greenleaf WJ, Block SM (2008) Single-molecule studies of RNA polymerase: motoring along. *Annu Rev Biochem* 77:149–76.

129. Grohmann D et al. (2011) The initiation factor TFE and the elongation factor Spt4/5 compete for the RNAP clamp during transcription initiation and elongation. *Mol Cell* 43:263–74.

130. Bai L, Santangelo TJ, Wang MD (2006) Single-molecule analysis of RNA polymerase transcription. *Annu Rev Biophys Biomol Struct* 35:343–60.

131. Larson MH et al. (2014) A pause sequence enriched at translation start sites drives transcription dynamics in vivo. *Science* 344:1042–7.

132. Galburt EA et al. (2007) Backtracking determines the force sensitivity of RNAP II in a factor-dependent manner. *Nature* 446:820–3.

133. Deniz AA, Mukhopadhyay S, Lemke EA (2008) Single-molecule biophysics: at the interface of biology, physics and chemistry. *J R Soc Interface* 5:15–45.

134. Roy R, Hohng S, Ha T (2008) A practical guide to single-molecule FRET. *Nat Methods* 5:507–16.

135. Weiss S (1999) Fluorescence Spectroscopy of Single Biomolecules. *Science (80-)* 283:1676–1683.

136. Friedman LJ, Mumm JP, Gelles J (2013) RNA polymerase approaches its promoter without long-range sliding along DNA. *Proc Natl Acad Sci U S A* 110:9740–5.

137. Jain A et al. (2011) Probing cellular protein complexes using single-molecule pull-down. *Nature* 473:484–8.

138. Hoskins AA, Gelles J, Moore MJ (2011) New insights into the spliceosome by single molecule fluorescence microscopy. *Curr Opin Chem Biol* 15:864–70.

139. Santoso Y et al. (2010) Conformational transitions in DNA polymerase I revealed by single-molecule FRET. *Proc Natl Acad Sci U S A* 107:715–20.

140. Hohlbein J et al. (2013) Conformational landscapes of DNA polymerase I and mutator derivatives establish fidelity checkpoints for nucleotide insertion. *Nat Commun* 4:2131.

141. Reyes-Lamothe R, Sherratt DJ, Leake MC (2010) Stoichiometry and architecture of active DNA replication machinery in Escherichia coli. *Science* 328:498–501.

142. Zhang Z, Revyakin A, Grimm JB, Lavis LD, Tjian R (2014) Single-molecule tracking of the transcription cycle by sub-second RNA detection. *Elife* 3:e01775.

143. Uphoff S, Reyes-Lamothe R, Garza de Leon F, Sherratt DJ, Kapanidis AN (2013) Single-molecule DNA repair in live bacteria. *Proc Natl Acad Sci U S A* 110:8063–8.

144. Lacowicz JR (2006) *Principles of fluorescence spectroscopy* (Springer).

145. Gell C, Brockwell D, Smith A (2006) *Handbook of Single Molecule Fluorescence Spectroscopy* (Oxford University Press).

146. McCann JJ, Choi UB, Zheng L, Weninger K, Bowen ME (2010) Optimizing methods to recover absolute FRET efficiency from immobilized single molecules. *Biophys J* 99:961–70.

147. Lee NK et al. (2005) Accurate FRET measurements within single diffusing biomolecules using alternating-laser excitation. *Biophys J* 88:2939–53.

148. Brooks Shera E, Seitzinger NK, Davis LM, Keller RA, Soper SA (1990) Detection of single fluorescent molecules. *Chem Phys Lett* 174:553–557.

149. Joo C, Balci H, Ishitsuka Y, Buranachai C, Ha T (2008) Advances in single-molecule fluorescence methods for molecular biology. *Annu Rev Biochem* 77:51–76.

150. Kapanidis AN et al. (2004) Fluorescence-aided molecule sorting: analysis of structure and interactions by alternating-laser excitation of single molecules. *Proc Natl Acad Sci U S A* 101:8936–41.

151. Chung HS, Louis JM, Eaton WA (2010) Distinguishing between protein dynamics and dye photophysics in single-molecule FRET experiments. *Biophys J* 98:696–706.

152. Benesch RE, Benesch R (1953) Enzymatic Removal of Oxygen for Polarography and Related Methods. *Science (80-)* 118:447–448.

153. Rasnik I, McKinney SA, Ha T (2006) Nonblinking and long-lasting single-molecule fluorescence imaging. *Nat Methods* 3:891–3.

154. Cordes T, Vogelsang J, Tinnefeld P (2009) On the mechanism of Trolox as antiblinking and antibleaching reagent. *J Am Chem Soc* 131:5018–9.

155. Greene EC, Wind S, Fazio T, Gorman J, Visnapuu M-L (2010) DNA curtains for high-throughput single-molecule optical imaging. *Methods Enzymol* 472:293–315.

156. Tinoco I, Gonzalez RL (2011) Biological mechanisms, one molecule at a time. *Genes Dev* 25:1205–31.

157. Sarkar SK, Bumb A, Mills M, Neuman KC (2013) SnapShot: single-molecule fluorescence. *Cell* 153:1408–1408.e1.

158. Myong S, Rasnik I, Joo C, Lohman TM, Ha T (2005) Repetitive shuttling of a motor protein on DNA. *Nature* 437:1321–5.

159. Pinkney JNM et al. (2012) Capturing reaction paths and intermediates in Cre-loxP recombination using single-molecule fluorescence. *Proc Natl Acad Sci U S A* 109:20871–6.

160. Berdis AJ (2009) Mechanisms of DNA polymerases. *Chem Rev* 109:2862–79.

161. Beese LS, Derbyshire V, Steitz TA (1993) Structure of DNA polymerase I Klenow fragment bound to duplex DNA. *Science* 260:352–5.

162. Korolev S, Nayal M, Barnes WM, Di Cera E, Waksman G (1995) Crystal structure of the large fragment of Thermus aquaticus DNA polymerase I at 2.5-A resolution: structural basis for thermostability. *Proc Natl Acad Sci U S A* 92:9264–8.

163. Kiefer JR et al. (1997) Crystal structure of a thermostable Bacillus DNA polymerase l large fragment at 2.1 Å resolution. *Structure* 5:95–108.

164. Li Y, Korolev S, Waksman G (1998) Crystal structures of open and closed forms of binary and ternary complexes of the large fragment of Thermus aquaticus DNA polymerase I: structural basis for nucleotide incorporation. *EMBO J* 17:7514–25.

165. Okumus B, Wilson TJ, Lilley DMJ, Ha T (2004) Vesicle encapsulation studies reveal that single molecule ribozyme heterogeneities are intrinsic. *Biophys J* 87:2798–806.

166. Okumus B, Arslan S, Fengler SM, Myong S, Ha T (2009) Single molecule nanocontainers made porous using a bacterial toxin. *J Am Chem Soc* 131:14844–9.

167. Holden SJ et al. (2010) Defining the limits of single-molecule FRET resolution in TIRF microscopy. *Biophys J* 99:3102–11.

168. Rhoades E, Gussakovsky E, Haran G (2003) Watching proteins fold one molecule at a time. *Proc Natl Acad Sci U S A* 100:3197–202.

169. Cisse I, Okumus B, Joo C, Ha T (2007) Fueling protein DNA interactions inside porous nanocontainers. *Proc Natl Acad Sci U S A* 104:12646–50.

170. Ha T, Tinnefeld P (2012) Photophysics of fluorescent probes for single-molecule biophysics and super-resolution imaging. *Annu Rev Phys Chem* 63:595–617.

171. Bhakdi S et al. (1996) Staphylococcal alpha-toxin, streptolysin-O, and Escherichia coli hemolysin: prototypes of pore-forming bacterial cytolysins. *Arch Microbiol* 165:73–9.

172. Chang CY, Niblack B, Walker B, Bayley H (1995) A photogenerated pore-forming protein. *Chem Biol* 2:391–400.

173. Zhou R, Kunzelmann S, Webb MR, Ha T (2011) Detecting intramolecular conformational dynamics of single molecules in short distance range with subnanometer sensitivity. *Nano Lett* 11:5482–8.

174. Jain A, Liu R, Xiang YK, Ha T (2012) Single-molecule pull-down for studying protein interactions. *Nat Protoc* 7:445–52.

175. Robb NC et al. (2012) The Transcription Bubble of the RNA Polymerase-Promoter Open Complex Exhibits Conformational Heterogeneity and Millisecond-Scale Dynamics: Implications for Transcription Start-Site Selection. *J Mol Biol*.

176. Treutlein B et al. (2012) Dynamic architecture of a minimal RNA polymerase II open promoter complex. *Mol Cell* 46:136–46.

177. Kim H, Tang G-Q, Patel SS, Ha T (2012) Opening-closing dynamics of the mitochondrial transcription pre-initiation complex. *Nucleic Acids Res* 40:371–80.

178. Belogurov GA et al. (2007) Structural basis for converting a general transcription factor into an operon-specific virulence regulator. *Mol Cell* 26:117–29.

179. Leibman M, Hochschild A (2007) A sigma-core interaction of the RNA polymerase holoenzyme that enhances promoter escape. *EMBO J* 26:1579–90.

180. Borukhov S, Goldfarb A (1993) Recombinant Escherichia coli RNA polymerase: purification of individually overexpressed subunits and in vitro assembly. *Protein Expr Purif* 4:503–11.

181. Kulbachinskiy A, Mustaev A (2006) Region 3.2 of the sigma subunit contributes to the binding of the 3'-initiating nucleotide in the RNA polymerase active center and facilitates promoter clearance during initiation. *J Biol Chem* 281:18273–6.

182. Margeat E et al. (2006) Direct observation of abortive initiation and promoter escape within single immobilized transcription complexes. *Biophys J* 90:1419–31.

183. Le Reste L, Hohlbein J, Gryte K, Kapanidis AN (2012) Characterization of dark quencher chromophores as nonfluorescent acceptors for single-molecule FRET. *Biophys J* 102:2658–68.

184. Uphoff S, Gryte K, Evans G, Kapanidis AN (2011) Improved temporal resolution and linked hidden Markov modeling for switchable single-molecule FRET. *Chemphyschem* 12:571–9.

185. Bronson JE, Fei J, Hofman JM, Gonzalez RL, Wiggins CH (2009) Learning rates and states from biophysical time series: a Bayesian approach to model selection and single-molecule FRET data. *Biophys J* 97:3196–205.

186. Gryte K (2012) Analysis Methods for Single Molecule Fluorescence Spectroscopy. Dissertation (University of Oxford).

187. Sanchez A, Osborne ML, Friedman LJ, Kondev J, Gelles J (2011) Mechanism of transcriptional repression at a bacterial promoter by analysis of single molecules. *EMBO J* 30:3940–6.

188. Cordes T et al. (2010) Sensing DNA opening in transcription using quenchable Förster resonance energy transfer. *Biochemistry* 49:9171–80.

189. Cámara B et al. (2010) T7 phage protein Gp2 inhibits the Escherichia coli RNA polymerase by antagonizing stable DNA strand separation near the transcription start site. *Proc Natl Acad Sci U S A* 107:2247–52.

190. Holstege FC, Timmers HT (1997) Analysis of open complex formation during RNA polymerase II transcription initiation using heteroduplex templates and potassium permanganate probing. *Methods* 12:203–11.

191. Liu X, Bushnell DA, Kornberg RD (2011) Lock and key to transcription: σ-DNA interaction. *Cell* 147:1218–9.

192. Ederth J, Artsimovitch I, Isaksson LA, Landick R (2002) The downstream DNA jaw of bacterial RNA polymerase facilitates both transcriptional initiation and pausing. *J Biol Chem* 277:37456–63.

193. Straney DC, Crothers DM (1985) Intermediates in transcription initiation from the E. coli lac UV5 promoter. *Cell* 43:449–459.

194. Straney DC, Crothers DM (1985) Intermediates in transcription initiation from the E. coli lac UV5 promoter. *Cell* 43:449–59.

195. Straney DC, Crothers DM (1987) Comparison of the open complexes formed by RNA polymerase at the Escherichia coli lac UV5 promoter. *J Mol Biol* 193:279–92.

196. Nickels BE, Mukhopadhyay J, Garrity SJ, Ebright RH, Hochschild A (2004) The sigma 70 subunit of RNA polymerase mediates a promoter-proximal pause at the lac promoter. *Nat Struct Mol Biol* 11:544–50.

197. Muschielok A et al. (2008) A nano-positioning system for macromolecular structural analysis. *Nat Methods* 5:965–71.

198. Harada Y et al. (2001) Direct observation of DNA rotation during transcription by Escherichia coli RNA polymerase. *Nature* 409:113–5.

199. Campbell EA et al. (2001) Structural Mechanism for Rifampicin Inhibition of Bacterial RNA Polymerase. *Cell* 104:901–912.

200. Schafer DA, Gelles J, Sheetz MP, Landick R (1991) Transcription by single molecules of RNA polymerase observed by light microscopy. *Nature* 352:444–8.

201. Ellinger T, Behnke D, Bujard H, Gralla JD (1994) Stalling of Escherichia coli RNA polymerase in the +6 to +12 region in vivo is associated with tight binding to consensus promoter elements. *J Mol Biol* 239:455–65.

202. Zenkin N, Severinov K (2004) The role of RNA polymerase sigma subunit in promoter-independent initiation of transcription. *Proc Natl Acad Sci U S A* 101:4396–400.

203. Pupov D et al. (2010) Multiple roles of the RNA polymerase {beta}' SW2 region in transcription initiation, promoter escape, and RNA elongation. *Nucleic Acids Res* 38:5784–96.

204. Zhang Y et al. (2014) GE23077 binds to the RNA polymerase "i" and "i+1" sites and prevents the binding of initiating nucleotides. *Elife* 3:e02450.

205. Greenfeld M, Pavlichin DS, Mabuchi H, Herschlag D (2012) Single Molecule Analysis Research Tool (SMART): an integrated approach for analyzing single molecule data. *PLoS One* 7:e30024.

206. Van Dijk M, Bonvin AMJJ (2009) 3D-DART: a DNA structure modelling server. *Nucleic Acids Res* 37:W235–9.